Coupled problems in analysis of quantum dots with multiband models

Prabhakar, S., Melnik, R., and Bonilla, L.

Proceedings of the Vth Conference on Computational Methods for Coupled Problems in Science and Engineering (Coupled Problems 2013), Eds.: S. Idelsohm, M. Papadrakakis, B. Schrefler, Spain, June 2013, ISBN: 978-84-941407-6-1, pp. 1120 - 1129, CIMNE, 2013.

V International Conference on Computational Methods for Coupled Problems in Science and Engineering
COUPLED PROBLEMS 2013
S. Idelsohn, M. Papadrakakis and B. Schrefler (Eds)

COUPLED PROBLEMS IN ANALYSIS OF QUANTUM DOTS WITH MULTIBAND MODELS

Sanjay Prabhakar* **and Roderick Melnik*,†**

*M^{2}NeT Laboratory, Wilfrid Laurier University
Waterloo, ON Canada, N2L 3C5

†Gregorio Millan Institute, Universidad Carlos III de Madrid,
Leganes, Spain, 28911

Key words: Finite Element Method, Coupled multiphysics problems, 8-band $\mathbf{k}\cdot\mathbf{p}$ method, Piezoelectric fields and potentials

Abstract. We investigate the influence of piezoelectromechanical effects on the band structures of electron (hole) states in wurtzite quantum dots. We apply the 8-band $\mathbf{k}\cdot\mathbf{p}$ method and solve the corresponding eigenvalue (partial differential equations) problem for quantum dots with wetting layers based on the Finite Element Method. The coupled multiphysics model includes the piezoelectromechanical part and the band structure calculation part for electrons (holes) in quantum dots. We show that the piezoelectromechanical effects bring the localization of electron states at the top of the dots and hole states at the bottom of the dots.

1 Introduction

Studies on low dimensional systems have attracted considerable attention, spurred on by the development of smaller and faster electronic devices and by the exploitation of their extraordinary properties for improved performance in various areas of science and technology, including nano- and micro-electronics, thermoelectricity and magnetism [1, 2, 3, 5]. Today's technology allows us to grow finite size semiconductor quantum dots with wetting layers. One can expect a straightforward analogy to the planar electronic/optoelectronic industry to extrapolate that complex compositionally modulated quantum dots structures could greatly increase the versatility and power of these building blocks in nanoscale applications [1, 2]. Low dimensional semiconductor nanostructures such as quantum dots, quantum wells and quantum wires can be grown in the laboratory by Stranski-Krastanov growth technique [1, 2, 3, 5, 6, 7, 8, 9, 10]. Devices based on these nanostructures are used in optoelectronics as light emitting diodes, lasers, etc [1, 2]. The band structures of nanostructures can be engineered and modified by several different schemes such as gate

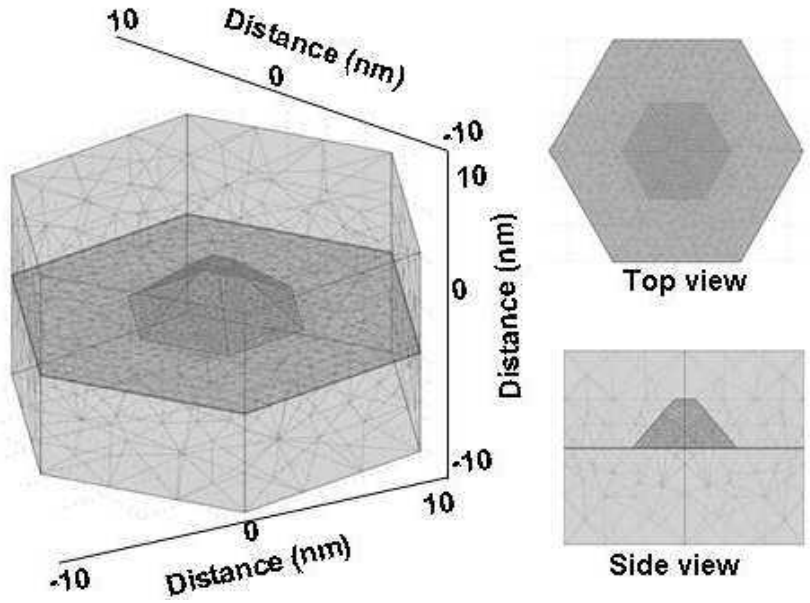

Figure 1: Realistic shape and size with actual mesh generated for an AlN/GaN quantum dot.

controlled electric fields and n- or p-type doped semiconductors as well as other techniques. Piezoelectromechanical effects provide another efficient way to modify the band diagram of semiconductor materials.

In this paper, based on the fully coupled model and 8-band $\mathbf{k} \cdot \mathbf{p}$ method, we analyze in detail the influence of electromechanical effects on the band structures of wurtzite GaN quantum dots with wetting layers.

2 Computational Method

We consider GaN quantum dots embedded into the AlN matrix of hexagon shape (see Fig. 1). In all results reported here, each side of the hexagon for AlN matrix has its length of 17 nm and height of 20 nm. The height of the pyramidal shape GaN wurtzite quantum dots is 5 nm. Such quantum dots are grown over 1 nm thickness of the wetting layer. In the first part of the solution procedure, we have solved the system of partial differential equations (PDEs) describing piezoelectromenchanical interactions in order to find the corresponding piezoelectric fields and potentials. In the second part, we diagonalize the strain dependent 8-band $\mathbf{k} \cdot \mathbf{p}$ Hamiltonian based on the Finite Element Method (FEM) [14]. In particular, in a typical simulation run, an AlN/GaN quantum dot with wetting layer contains the total number of 15945 elements, of which (from bottom to top) 4698 elements are in the lower barrier, 4255 elements are in the wetting layer, 3615 elements are in the quantum dots, and 3377 elements are in the upper barrier (see Fig. 1). We impose the Neumann boundary condition at the interface of AlN/GaN and the Dirichlet boundary conditions on the rest of the boundary. We utilize the UMFPACK solver in the

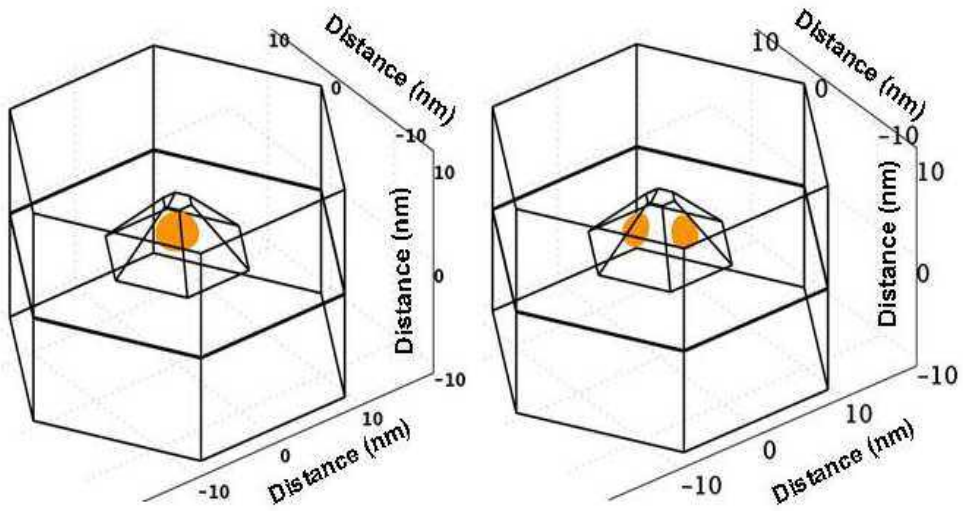

Figure 2: (Color online) Probability distributions of ground and first excited states of electrons in an AlN/GaN quantum dot without accounting for piezoelectromechanical effects.

COMSOL multiphysics package [14] to find the piezoelectromechanical fields, eigenvalues and eigenfunctions of the corresponding eigenvalue PDE problem. Following [11, 12], in the next section we provide further details on the Hamiltonian and two main parts of the mathematical model.

3 Physics-Based Mathematical Model

3.1 Piezoelectromechanical effects in Cartesian coordinates

The starting point for the analysis of the influence of piezoelectromechanical effect on the band structure calculation of low dimensional semiconductor nanostructures is the coupled system of the Navier equations for stress and Maxwel's equations for piezoelectric fields as [11]

$$\partial_j \sigma_{ik} = 0, \tag{1}$$

$$\partial_i D_i = 0. \tag{2}$$

The stress tensor components σ_{ik} and the electric displacement vector components D_i are given by

$$\sigma_{ik} = C_{iklm}\varepsilon_{lm} + e_{nik}\partial_n V, \tag{3}$$

$$D_i = e_{ilm}\varepsilon_{lm} - \hat{\epsilon}_{in}\partial_n V + P_{sp}\delta_{iz}, \tag{4}$$

where C_{iklm} are the elastic moduli constants, e_{ik} is the piezoelectric constant, ϵ_{in} is the permittivity, V is the piezoelectric potential, P_{sp} is the spontaneous polarization and

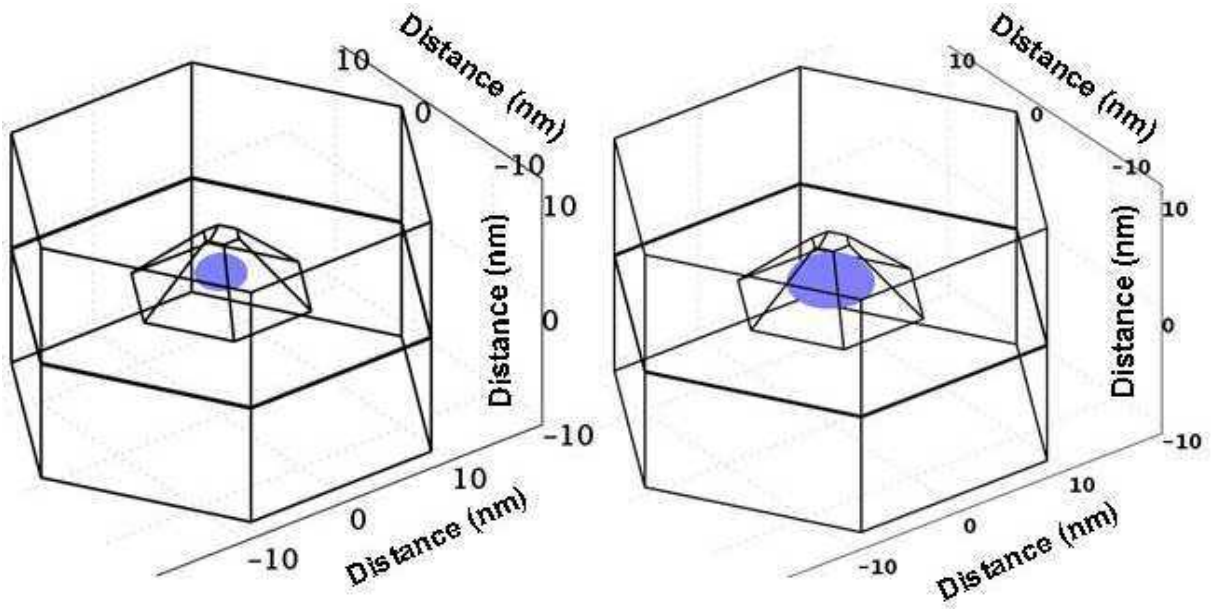

Figure 3: (Color online) Probability distributions of heavy holes and light holes in an AlN/GaN quantum dot without accounting for piezoelectromechanical effects.

$E = -\frac{\partial V}{\partial z}$ is the built in piezoelectric field. Also, ε_{ik} are the components of strain tensors which are written as

$$\varepsilon_{ij} = \varepsilon_{ij}^{u} + \varepsilon_{ij}^{0}, \tag{5}$$

where ε_{ij}^{0} are the local intrinsic strain tensor components due to lattice mismatch and ε_{ij}^{u} is position dependent strain tensor components. These two can be written as

$$\varepsilon_{ij}^{0} = \left(\delta_{ij} - \delta_{iz}\delta_{jz}\right) a + \delta_{iz}\delta_{jz} c, \tag{6}$$

$$\varepsilon_{ij}^{u} = \frac{1}{2}\left(\partial_j u_i + \partial_i u_j\right), \tag{7}$$

where $a = \left(a_0 - a\right)/a_0$ and $c = \left(c_0 - c\right)/c_0$ are the local intrinsic strains along a- and c-directions, respectively (which are nonzero in the quantum dots and zero otherwise). Here, a_0, c_0 and a, c are the lattice constants of the quantum dots and the barrier material of the NWSLs.

3.2 8-band $\mathbf{k}\cdot\mathbf{p}$ model in Cartesian coordinates

The steady state Schrödinger equation of the Kane model for the electrons in the conduction band and holes in the valence band can be written as [11]

$$\mathbf{H}\boldsymbol{\psi} = E\boldsymbol{\psi}, \tag{8}$$

where

$$\mathbf{H} = \begin{pmatrix} \mathbf{H_c} & \mathbf{H_{cv}} \\ \mathbf{H_{cv}^{\dagger}} & \mathbf{H_v} \end{pmatrix}, \boldsymbol{\psi} = \begin{pmatrix} \boldsymbol{\psi_c} \\ \boldsymbol{\psi_v} \end{pmatrix}, \tag{9}$$

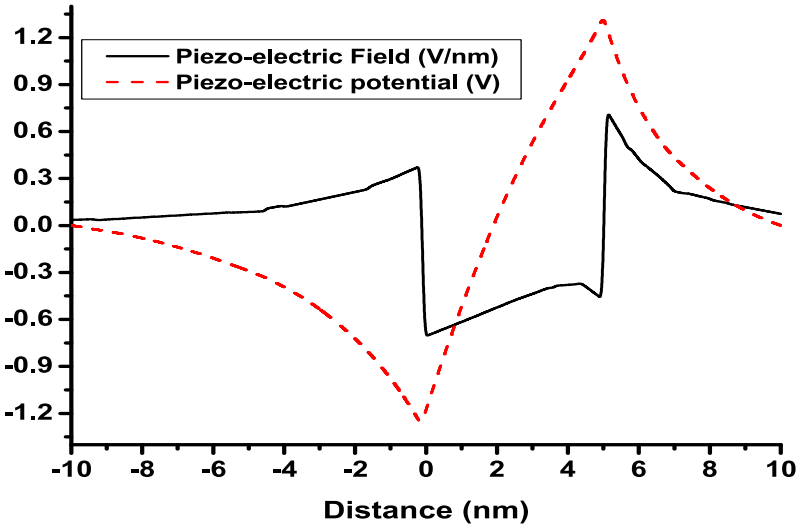

Figure 4: (Color online) Piezoelectric field and piezoelectric potential vs distance along z-direction in an AlN/GaN quantum dot.

with $\boldsymbol{\psi_c} = \boldsymbol{\psi_c}(\mathbf{r})$ and $\boldsymbol{\psi_v} = \boldsymbol{\psi_v}(\mathbf{r})$ are the position dependent conduction and valence band envelope function.

The total wave function $\boldsymbol{\Psi}$ is (see [11])

$$\boldsymbol{\Psi} = \sum_{j=c,x,y,z} f_j \psi_j = \boldsymbol{f}\boldsymbol{\psi}, \tag{10}$$

where $\boldsymbol{f} = (f_c\ f_x\ f_y\ f_z)$ and $\boldsymbol{\psi} = (\boldsymbol{\psi_c}\ \boldsymbol{\psi_x}\ \boldsymbol{\psi_y}\ \boldsymbol{\psi_z})^{\boldsymbol{T}}$. The functions $\boldsymbol{f}$ are spinless and $\boldsymbol{\psi}$ is a spinor:

$$\boldsymbol{\psi_j} = \begin{pmatrix} \psi_j^1 \\ \psi_j^2 \end{pmatrix}, \quad j = c, x, y, z. \tag{11}$$

Hence, the basis functions of the Hamiltonian (9) take the following form:

$$\left(f_c\psi_c^1,\ f_c\psi_c^2,\ f_x\psi_x^1,\ f_x\psi_x^2,\ f_y\psi_y^1,\ f_y\psi_y^2,\ f_z\psi_z^1,\ f_z\psi_z^2\right)^T$$

The next step is the description of the matrix Hamiltonian $\mathbf{H}$ of (9). The diagonal element of the conduction band Hamiltonian $\mathbf{H_c}$ can be written as

$$\begin{aligned} H_c = \ & A_1' k_z^2 + A_2' \left(k_x^2 + k_y^2\right) + U_c \\ & + a_1 \varepsilon_{zz} + a_2 \left(\varepsilon_{xx} + \varepsilon_{yy}\right), \end{aligned} \tag{12}$$

where $U_c = U_c(\mathbf{r})$ is the position dependent edge of the conduction band Γ_1, a_1 and a_2 are deformation potentials for the conduction band. The parameters A_1' and A_2' are expressed

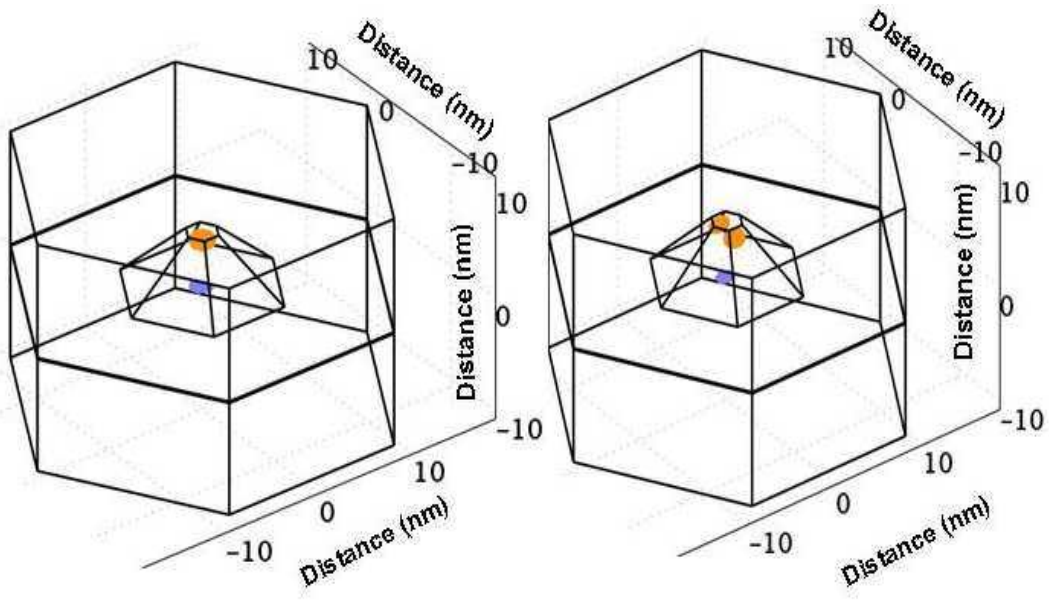

Figure 5: (Color online) Probability distributions of ground and first excited states of electrons (holes) in an AlN/GaN quantum dot with piezoelectromechanical effects. Notice that the piezoelectromechanical effects bring the localization of electron wavefunctions to the top of the dot and hole wavefunctions to the bottom of the dot.

via the components $1/m_{\parallel}$ and $1/m_{\perp}$ of the tensor of the reciprocal effective masses for the conduction band in the single-band approximation and the Kane parameters $P_1 = -i\hbar\langle\phi_c|\hbar k_z|\phi_z\rangle/m_0$ and $P_2 = -i\hbar\langle\phi_c|\hbar k_x|\phi_x\rangle/m_0$. They are given by [11]

$$A_1' = \frac{\hbar^2}{2m_{\parallel}} - \frac{P_1^2}{E_g}, \tag{13}$$

$$A_2' = \frac{\hbar^2}{2m_{\perp}} - \frac{P_2^2}{E_g}, \tag{14}$$

where E_g is the band gap of semiconductor materials.

The intra-valence-band Hamiltonian $\mathbf{H_v}$ can be written as

$$\mathbf{H_v} = \mathbf{H^{(0)}} + \mathbf{H^{(so)}} + \mathbf{H^{(\varepsilon)}} + \mathbf{H'^{(k)}}. \tag{15}$$

The Hamiltonian $\mathbf{H^{(0)}}$ entering Eq. (15) represents the position-dependent potential energy of an electron:

$$\mathbf{H^{(0)}} = \begin{pmatrix} U_{v6} & 0 & 0 \\ 0 & U_{v6} & 0 \\ 0 & 0 & U_{v1} \end{pmatrix}, \tag{16}$$

where $U_{v6} = U_{v6}(\mathbf{r})$ and $U_{v1} = U_{v1}(\mathbf{r})$ are the position dependent edges of the valence bands Γ_6 and Γ_1, respectively.

The spin-orbit Hamiltonian $\mathbf{H}^{(\mathbf{so})}$ in Eq. (15) can be treated as a perturbation term and can be written as [7, 8]

$$\mathbf{H}^{(\mathbf{so})} = i \begin{pmatrix} 0 & -\Delta_2\sigma_z & \Delta_3\sigma_y \\ \Delta_2\sigma_z & 0 & -\Delta_3\sigma_x \\ -\Delta_3\sigma_y & \Delta_3\sigma_x & 0 \end{pmatrix}, \tag{17}$$

where $\Delta_2 = \Delta_2(\mathbf{r})$ and $\Delta_3 = \Delta_3(\mathbf{r})$ are the parameters of the valence-band spin-orbit splitting and $\sigma_i (i = x, y, z)$ are the Pauli spin matrices:

$$\sigma_x = \begin{pmatrix} 0 & 1 \\ 1 & 0 \end{pmatrix}, \ \sigma_y = \begin{pmatrix} 0 & -i \\ i & 0 \end{pmatrix}, \ \sigma_z = \begin{pmatrix} 1 & 0 \\ 0 & -1 \end{pmatrix}. \tag{18}$$

The kinetic energy Hamiltonian $\mathbf{H}^{\prime(\mathbf{k})}$ in Eq. (15) can be written as

$$\mathbf{H}^{\prime(\mathbf{k})} = \begin{pmatrix} L_1'k_x^2 + M_1k_y^2 + M_2k_z^2 & N_1'k_xk_y & N_2'k_xk_z \\ N_1'k_xk_y & M_1k_x^2 + L_1'k_y^2 + M_2k_z^2 & N_2'k_yk_z \\ N_2'k_xk_z & N_2'k_yk_z & M_3\left(k_x^2 + k_y^2\right) + L_2'k_z^2 \end{pmatrix}, \tag{19}$$

where

$$L_1' = L_1 + \frac{P_1^2}{E_g}, \quad L_2' = L_2 + \frac{P_2^2}{E_g}, \tag{20}$$

$$N_1' = N_1 + \frac{P_1^2}{E_g}, \quad N_2' = N_2 + \frac{P_1P_2}{E_g}. \tag{21}$$

Also,

$$\begin{aligned} L_1 &= \frac{\hbar^2}{2m_0}\left(A_2 + A_4 + A_5\right), \\ M_1 &= \frac{\hbar^2}{2m_0}\left(A_2 + A_4 - A_5\right), \\ N_1 &= \frac{\hbar^2}{2m_0}2A_5, \quad L_2 = \frac{\hbar^2}{2m_0}A_1, \\ M_2 &= \frac{\hbar^2}{2m_0}\left(A_1 + A_3\right), \quad N_2 = \frac{\hbar^2}{2m_0}\sqrt{2}A_6 \\ M_3 &= \frac{\hbar^2}{2m_0}A_2, \quad N_3 = i\sqrt{2}A_7, \end{aligned} \tag{22}$$

with $A_1, A_2, \ldots A_7$ being real material parameters in conventional notations [7, 8, 11], m_0 is the free electron mass. Wurtzite structure has six fold rotational symmetry and thus we use the relation $L_1' - M_1 = N_1'$.

Finally, the strain tensor components are written as [11]

$$\mathbf{H}^{(\varepsilon)} = \begin{pmatrix} l_1\varepsilon_{xx} + m_1\varepsilon_{yy} + m_2\varepsilon_{zz} & n_1\varepsilon_{xy} & n_2\varepsilon_{xz} \\ n_1\varepsilon_{xy} & m_1\varepsilon_{xx} + l_1\varepsilon_{yy} + m_2\varepsilon_{zz} & n_2\varepsilon_{yz} \\ n_2\varepsilon_{xz} & n_2\varepsilon_{yz} & m_3\left(\varepsilon_{xx} + \varepsilon_{yy}\right) + l_2\varepsilon_{zz} \end{pmatrix}, \quad (23)$$

where material constants l_1, l_2 m_1, m_2, n_1, and n_2 are expressed via conventional deformation potential tensor components as follows: [8, 7, 11]

$$\begin{aligned} &l_1 = D_2 + D_4 + D_5, \quad m_1 = D_2 + D_4 - D_5, \\ &n_1 = 2D_5, \quad l_2 = D_1, \quad m_2 = D_1 + D_3, \\ &n_2 = \sqrt{2}D_6, \quad m_3 = D_2. \end{aligned} \quad (24)$$

We can also apply six fold rotational symmetry in the strain Hamiltonian of wurtzite structure which holds the relation $l_1 - m_1 = n_1$.

The Hamiltonian $\mathbf{H_{cv}}$ of (9) ($\mathbf{H_{cv}^{\dagger}}$ is its Hermitian conjugate) can be written as

$$\mathbf{H_{cv}} = \left(H_{cx} \;\; H_{cy} \;\; H_{cz}\right), \quad (25)$$

where

$$H_{cx} = iP_2k_x, \quad H_{cy} = iP_2k_y, \quad H_{cz} = \; iP_1k_z. \quad (26)$$

4 Results and Discussions

In Fig. 2, we have plotted the probability distributions of ground and first excited states of electrons in AlN/GaN quantum dots without accounting for piezoelectromechanical effects. In Fig. 3, we have plotted the probability distributions of heavy holes and light holes in AlN/GaN quantum dots without accounting for piezoelectromechanical effects. Since we consider the flat band of AlN/GaN quantum dots in our 8-band $\mathbf{k}\cdot\mathbf{p}$ Hamiltonian, we see that the localization of the wave functions of the electrons and holes in quantum dots reside in the center of the dots.

Next, we have solved the piezoelectromechanical part and plotted the piezoelectric fields and piezoelectric potentials in AlN/GaN quantum dots in Fig. 4. We couple the piezoelectromechanical and band structure calculation parts via the 8-band $\mathbf{k}\cdot\mathbf{p}$ Hamiltonian.

Then, we have diagonalized the strain dependent 8-band $\mathbf{k}\cdot\mathbf{p}$ Hamiltonian based on Finite Element Method and investigate the influence of piezoelectromechanical effects in wurtzite AlN/GaN quantum dots. In Fig. 5, we have plotted the probability distributions of ground and first excited states of electrons and holes in AlN/GaN quantum dots. It can be seen that the influence of piezoelectromechanical effects bring the electron states to the top of the dots and hole states (both heavy and light holes) to the bottom of the dots near the wetting layers.

5 Conclusion

We have solved the three-dimensional coupled multiphysics model of strain dependent 8-band $\mathbf{k} \cdot \mathbf{p}$ Hamiltonian in Cartesian coordinates based on the Finite Element Method. We have shown that without piezoelectromechanical effects, electron and hole wavefunctions are located in the center of the quantum dots. By accounting for piezoelectromechanical effects, we have found that in the analyzed wurtzite AlN/GaN quantum dots these effects push the distribution of electron wavefunctions to the top of the quantum dots and hole wavefunctions to the bottom of the quantum dots, near the wetting layer.

6 Acknowledgement

This work was supported by Natural Sciences and Engineering Research Council (NSERC) of Canada and Canada Research Chair (CRC) programs.

REFERENCES

[1] L. Jacak, P. Hawrylak, and A. Wójs, *semiconductor quantum dots* (Berlin : Springer, 1998).

[2] P. Harrison, *Quantum Wells, Wires and Dots* (John Wiley & Sons, Ltd, 2006).

[3] O. Marquardt,D. Mourad, S. Schulz, T. Hickel, G. Czycholl and J. Neugebauer, Comparison of atomistic and continuum theoretical approaches to determine electronic properties of GaN/AlN quantum dots *Phys. Rev. B* **78**, 235302 (2008).

[4] S. Prabhakar and R. Melnik, Influence of electromechanical effects and wetting layers on band structures of AlN/GaN quantum dots and spin control *Journal of Applied Physics* **108**, 064330 (2010).

[5] X. Peng, L. Manna, W. Yang, and J. Wickham, E. Scher, A. Kadavanich and A. P. Alivisatos, Shape control of CdSe nanocrystals *Nature* **404**, 59 (2000).

[6] S. Tanaka, S. Iwai and Y. Aoyagi, Self-assembling GaN quantum dots on $Al_xGa_{1-x}N$ surfaces using a surfactant *Applied Physics Letters* **69**, 4096 (1996).

[7] S. L. Chuang and C. S. Chang, "Self-assembling GaN quantum dots on $k \cdot p$ method for strained wurtzite semiconductors *Phys. Rev. B* **54**, 2491 (1996).

[8] G.L. Bir and G.E. Pikus, *Symmetry and strain induced effects in semiconductors* (Wiley, 1974).

[9] L.D. Landau and E.M. Lifshitz, *Theory of Elasticity* (Pergamon Press, Oxford, 1970).

[10] A. H. Meitzler, *IEEE Standard on Piezoelectricity*(IEEE Press, 1987).

[11] S. Prabhakar, R. Melnik, P. Neittaanmäki, and T. Tiihonen,, Coupled electromechanical effects in wurtzite quantum dots with wetting layers in gate controlled electric fields: The multiband case, *Physica E* **46**, 97-104 (2012). (2012).

[12] S. Prabhakar, R. Melnik, P. Neittaanmäki, and T. Tiihonen, Coupled magneto-thermoelectromechanical effects and electronic properties of quantum dots, *Journal of Computational and Theoretical Nanoscience* **10**, 550-563 (2013).

[13] B. Lassen, M. Willatzen, D. Barettin, R. V. N. Melnik, and L. C. L. Y. Voon, Electromechanical effects in electron structure for GaN/AlN quantum dots, *Journal of Physics: Conference Series* **107**, 012008 (2008).

[14] Comsol Multiphysics version 3.5a (www.comsol.com).